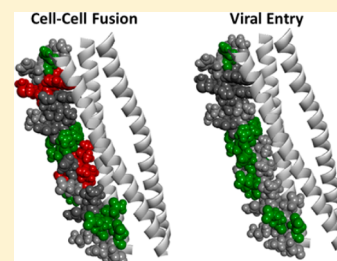


# Significant Differences in Cell–Cell Fusion and Viral Entry between Strains Revealed by Scanning Mutagenesis of the C-Heptad Repeat of HIV gp41

Barbara Diaz-Aguilar, Karen DeWispelaere, Hyun Ah Yi, and Amy Jacobs\*

Department of Microbiology and Immunology, School of Medicine and Biomedical Sciences, University at Buffalo, The State University of New York, Buffalo, New York 14214, United States

**ABSTRACT:** The transmembrane subunit, gp41, of the HIV envelope mediates the viral fusion step of entry into the host cell. The protein consists of an extracellular domain, a transmembrane domain, and a cytoplasmic tail. The extracellular domain contains a fusion peptide, an N-terminal heptad repeat, a loop region, a C-terminal heptad repeat (CHR), and a membrane-proximal external region. For this study, we examined each amino acid in the CHR (residues 623–659) by alanine scanning mutagenesis in two HIV strains: one CCR5-utilizing strain (JRFL) and one CXCR4-utilizing strain (HXB2). We studied the functional importance of each amino acid residue by measuring mutational effects in both cell–cell fusion and viral entry and assessing envelope expression and gp120–gp41 proteolytic processing. The transmembrane subunit of the HIV envelope, gp41, is very sensitive to subtle changes, like alanine substitution, which severely affect envelope function at multiple sites. Two important general findings are apparent when the entire data set from this study is taken into account. (1) Strain HXB2 is much more stable to mutagenesis than strain JRFL, and (2) viral entry is much more stable to mutagenesis than cell–cell fusion. These findings strengthen our notion that gp41 is a vulnerable target for therapeutic and prophylactic intervention. Further structural studies aimed at gaining a full understanding of the intermediate states that drive HIV membrane fusion are imperative.



Infection by human immunodeficiency virus type 1 (HIV-1) is initiated when the virus particle makes contact with the receptor cell surface; subsequently, HIV envelope gp41 mediates membrane fusion, thereby allowing the viral genetic material to enter the cell. The HIV-1 envelope glycoprotein is synthesized as a precursor polypeptide, gp160, which is proteolytically processed by the cellular protease, furin, to generate two subunits, the surface subunit gp120 (sometimes termed SU) and the transmembrane subunit gp41 (sometimes termed TM). These subunits are noncovalently associated and form a trimer of heterodimers that is the envelope glycoprotein spike on the viral surface. Initial contact with the host cell is made when gp120 interacts with CD4. Conformational changes allow subsequent binding of gp120 to a chemokine coreceptor (CCR5 or CXCR4) found on the surface of target cells. These events trigger gp41 to undergo conformational changes that are crucial for activation of HIV-1 membrane fusion. HIV-1 fusion likely involves substantial conformational changes in gp41, going from a metastable state to an energetically more stable conformation.<sup>1–4</sup> The control of these structural rearrangements is thought to be central to HIV-1 entry and an important target for drug development, proven by the therapeutic use of the fusion inhibitor (T20/Fuzeon/Enfuvirtide).<sup>5–7</sup>

Structural studies have demonstrated that the N-terminal heptad repeat (NHR) and C-terminal heptad repeat (CHR) regions of the gp41 ectodomain associate to form a six-helix bundle in the postfusion state with three N-terminal helices forming a trimeric coiled coil in the center and three C-terminal helices packing on the surface of the coiled coil in a reverse

orientation resembling a hairpinlike structure.<sup>8–14</sup> This transition is concomitant with membrane fusion.<sup>15,16</sup> The transmembrane region is positioned in the viral membrane, and the fusion peptide is embedded in the cellular membrane after gp120 makes contact with the cellular receptors. Intermediate states of the gp41 molecule are vital to viral function, and the regions involved are highly conserved. Hence, they serve as a target for the development of HIV-1 inhibitors.

There is evidence that packing interactions between the NHR and CHR are important determinants of HIV-1 entry.<sup>5,17–19</sup> The receptor-triggered conformational changes in the HIV-1 envelope glycoprotein that result in the formation of the stable gp41 core are suspected to drive the increasing proximity of the membranes and/or the subsequent lipid bilayer fusion.<sup>16</sup> Therefore, it is of fundamental importance to understand the structural and mechanistic basis for the interactions in the core.

The CHR is a functionally important region in HIV gp41 that forms a part of the postfusion six-helix bundle (6HB) structure of gp41. The 6HB conformation of gp41 is a stable trimer in which the NHR forms an internal three-helix bundle and the CHR wraps obliquely around the internal bundle to form the 6HB.<sup>8–10,13,20,21</sup> In this study, alanine substitutions at 37 positions within the CHR have been characterized in two different HIV-1 strains, one CCR5-utilizing strain (JRFL) and

**Received:** February 15, 2013

**Revised:** April 25, 2013

**Published:** April 26, 2013



one CXCR4-utilizing strain (HXB2). We have studied these mutations for effects on membrane fusion, viral entry, envelope expression, furin cleavage, and gp41–gp120 association. We used alanine substitutions because alanine is considered one of the most subtle single-amino acid changes that can be made with respect to chemical character and molecular structure but which also does not add backbone flexibility, as would be the case with glycine substitution. We present a systematic mutagenesis approach to studying the importance of each amino acid residue of the CHR region to gp41 function in two different HIV-1 strains, one CCR5-utilizing strain (JRFL) and one CXCR4-utilizing strain (HXB2), with the long-term goal of identifying regions that are attractive sites for drug intervention and are amenable to manipulation for labeling for structural studies.

The mechanisms of cell–cell fusion and viral entry have historically been considered to be substantially similar following the same steps of (1) attachment of gp120 to CD4 on the cell surface, (2) conformational changes in gp120 leading to coreceptor binding, and (3) further conformational changes in gp41 mediating membrane fusion at the plasma membrane. Interestingly, however, recent studies have convincingly demonstrated that HIV entry occurs through the endocytic pathway.<sup>16,22</sup> This alteration to the paradigm of HIV viral entry suggests that the mechanistic difference between cell–cell fusion and viral entry might also be greater than originally thought. Membrane fusion is required for both phenomena; however, different membranes are now implicated, with the plasma membrane being the site of cell–cell fusion and the endocytic membrane being the membrane that must fuse with the viral membrane for viral entry of the core. It is not yet clear what restricts the virion from fusing with the plasma membrane. It is known, however, that dynamin is required for HIV entry, which implicates the clathrin-dependent pathway.<sup>16,22</sup> There is a difference in the amount of membrane curvature between the two mechanisms. The region of membrane fusion between two cells is often considered to have so little curvature that it can be estimated as a plane, whereas the curvature of the viral membrane is much greater and more closely matches the curvature of the endosomal membrane than the curvature of the plasma membrane. There is also a possibility that there are different concentrations of host cell proteins in the environment in which membrane fusion is taking place, and this could have an effect on the two processes.

Interestingly, we found the effects of mutagenesis on cell–cell fusion versus viral entry to vary substantially in some cases. This would suggest that there are key differences in the mechanisms between these two phenomena. In fact, researchers had found evidence to suggest this in previous studies. For instance, Konopka et al. found that there was a difference in monoclonal antibody binding between cell–cell fusion and virus–cell membrane fusion with a murine monoclonal antibody (mAb F-91–55) raised against the complex of CD4 and gp120.<sup>23</sup> In another study, additional monoclonal antibodies were found to be relatively ineffective at inhibiting cell–cell fusion as well.<sup>24</sup> Antibodies b12, m14 IgG, and 2G12 had moderate activity, whereas 4E10 and 2F5 that bind the membrane-proximal region of gp41 had no inhibitory effect.<sup>24</sup> Further study to elucidate differences between the mechanisms of cell–cell fusion and viral entry in HIV-1 biology is warranted.

## MATERIALS AND METHODS

**Plasmids and Mutagenesis.** The plasmids bearing alanine substitutions were prepared from pHXB2 [National Institutes of Health (NIH) AIDS Research and Reference Reagent Program catalog no. 526]<sup>25</sup> and pJRFL that, to match the background of pHXB2, was cloned into the pSV7D background plasmid from pCAGGSJRFL (a gift from J. M. Binley).<sup>26</sup> Mutagenesis was performed using the Stratagene QuikChange II XL site-directed mutagenesis kit, and changes were verified by DNA sequencing (Roswell Park Cancer Institute DNA Sequencing Laboratory). The plasmid expressing Rev was pCMV-rev (pRev-1) (NIH AIDS Research and Reference Reagent Program catalog no. 1443),<sup>27</sup> and the plasmid expressing Tat was pCEP4-Tat (NIH AIDS Research and Reference Reagent Program catalog no. 4691).<sup>28</sup>

**Cell–Cell Fusion.** For the cell–cell fusion assay, envelope plasmid pHXB2 or pJRFL, wild type (WT) or each mutant, was cotransfected with plasmids for both Tat and Rev viral proteins by precipitation of calcium phosphate into 293T cells (ATCC), maintained in Dulbecco's modified Eagle's medium (DMEM) with 10% fetal bovine serum (FBS) and 1% penicillin/streptomycin. Twenty-four hours post-transfection, the cells were removed from the plate, counted, and then seeded at a density of  $2 \times 10^4$  cells/well along with  $2 \times 10^4$  cells/well of the receptor cell line, TZM-bl (NIH AIDS Research and Reference Reagent Program catalog no. 8129),<sup>29</sup> into a 96-well plate. The plates were incubated overnight at 37 °C in a 5% CO<sub>2</sub> incubator. After 24 h, membrane fusion levels were measured by a luciferase assay (One-glo, Promega) according to the manufacturer's protocol using the Spectra Max M5 (Molecular Devices) plate reader, and levels were normalized to the WT fusion levels. Experiments were performed in triplicate from the transfection step to the measurement of luciferase activity; thus, the uncertainties are inclusive of all steps of the experimental procedure.

**Viral Entry.** For the viral entry assay, plasmids pHXB2 or pJRFL, WT and each mutant, and pNL4-3.HSA.R-E- (NIH AIDS Research and Reference Reagent Program catalog no. 3417)<sup>30</sup> were cotransfected by calcium phosphate precipitation into 293T cells, which were maintained in DMEM with 10% FBS and 1% penicillin/streptomycin. Forty-eight hours post-transfection, the medium was harvested and filtered through a 0.45 µm filter and centrifuged at 55000g for 1 h to make the virus stock. The infectious titer of the wild-type (WT) virus was measured by X-gal staining as previously described.<sup>31</sup> The HIV-1 p24 antigen capture enzyme-linked immunoassay (AIDS & Cancer virus program, National Cancer Institute at Frederick, Frederick, MD) was performed to determine equivalent amounts of mutant envelope viral particles to WT virus at a multiplicity of infection (MOI) of 0.01. Then the amount of p24 at an MOI of 0.01 of WT was utilized to normalize for viral particle number, and a p24 concentration of each mutated virus of 100 ng/mL was used throughout the work. The receptor cells, TZM-bl, which were maintained in DMEM with 10% FBS and 1% penicillin/streptomycin, were seeded at a density of  $2 \times 10^4$  cells/well in a 96-well plate in a volume of 100 µL. The following day, the medium was removed and 100 µL of the virus stock (MOI of 0.01, 100 ng/mL p24) was added to each of the wells. The plates were centrifuged at 3000g for 1 h and then incubated at 37 °C in a 5% CO<sub>2</sub> incubator. After 48 h, viral entry levels were measured by a luciferase assay as described above for the cell–cell fusion assay.

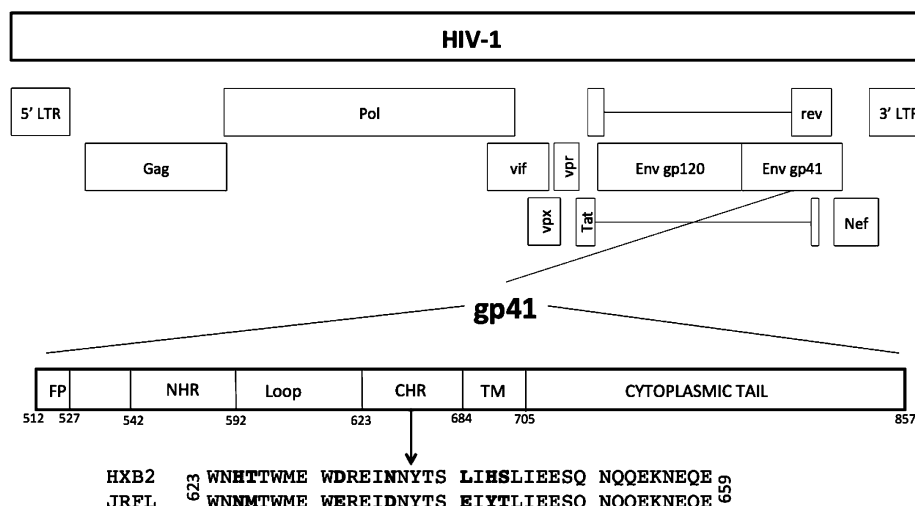


**Figure 1.** Diagram of the HIV genome, with an emphasis on the CHR domain of the envelope transmembrane subunit, gp41. Amino acids that are not conserved between the two strains are shown in bold.

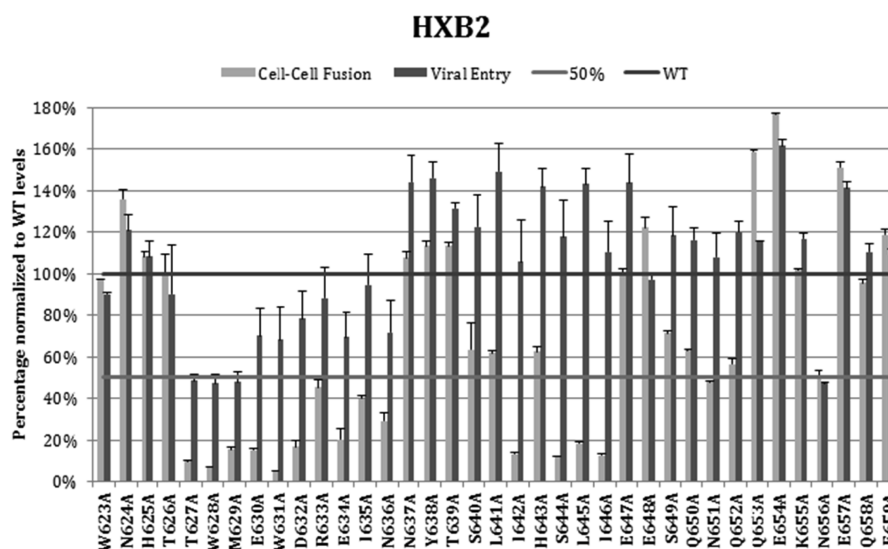


**Figure 2.** Levels of cell–cell fusion and viral entry substitutions in the CHR region of strain HXB2. The results are presented as a percentage of the luciferase signal normalized to the WT level. The error bars represent the standard deviation of three separate experiments.

**Protein Quantification.** The virus pellet was prepared by ultracentrifugation at 55000 rpm for 1 h using a Beckman SW55Ti rotor. The pellets were resuspended in lysis buffer [50 mM Tris (pH 7.5), 150 mM NaCl, 5 mM EDTA, 0.5% Nonidet P-40, and 0.1% SDS]. The 293T cell lysates were collected using M-Per mammalian protein extraction reagent (Thermo Scientific). Cell lysates and virus pellets were normalized for total protein concentration using the BCA protein assay kit (Pierce).

**Western Blot Analysis.** After electrophoresis, transfer, and blocking, the blots were probed with mouse anti-HIV-1 gp41 monoclonal antibody (Chessie 8; NIH AIDS Research and Reference Reagent Program catalog no. 526)<sup>32</sup> and the anti-HIV-1 gp120 polyclonal antibody (U.S. Biologicals). To ensure that the virus stock contains equal amounts of virus particles, normalization was performed on the basis of Western blots for p24 levels using the anti-HIV-1 p24 monoclonal antibody (NIH AIDS Research and Reference Reagent Program). The total protein concentration was determined using the BCA assay as described above, and 10  $\mu$ g of total protein was loaded

per lane. The secondary antibody used was IR800-conjugated donkey anti-mouse IgG for gp41 and p24 and IR700-conjugated rabbit anti-goat IgG for gp120, and blots were scanned and analyzed using the Odyssey Infrared Imaging System (LI-COR).

## RESULTS

**Design of gp41 CHR Mutational Scanning.** On the basis of structural studies and the HIV genome, the CHR consists of 37 residues (623–659) in the HIV-1 HXB2 envelope sequence. In the sequence from the amino terminus to the carboxy terminus, the gp41 subunit is divided into the fusion peptide, the NHR, the loop region, CHR, the transmembrane region, and the cytoplasmic tail (Figure 1). Of the 37 residues that constitute the CHR, 30 are conserved between the two strains tested in this study, HXB2 and JRFL, which yields an overall level of sequence identity of 85%.

**Cell–Cell Fusion and Viral Entry of gp41 CHR Substitutions.** The effects of scanning mutagenesis on cell–cell fusion were assayed by a luciferase-based assay in which the



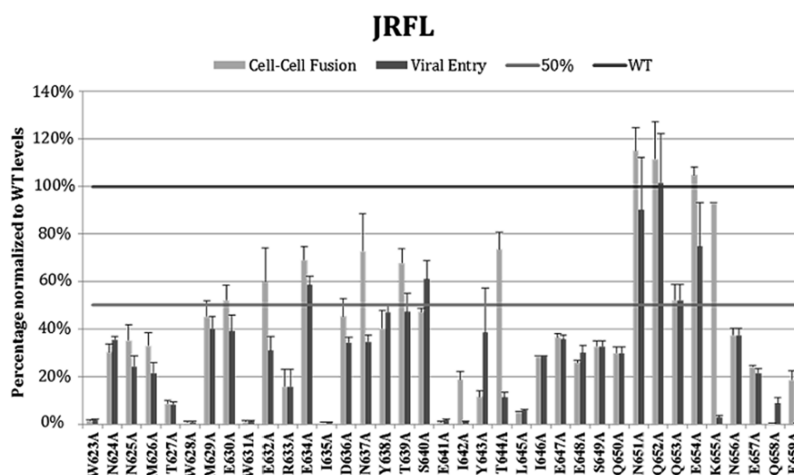


**Figure 3.** Levels of cell–cell fusion and viral entry substitutions in the CHR region of strain JRFL. The results are presented as a percentage of the luciferase signal normalized to the WT level. The error bars represent the standard deviation of three separate experiments.

core containing the genetic material of the virus can enter the cytoplasm only upon membrane fusion of the plasma membrane of the receptor cell line with the plasma membrane of the cell line containing the envelope complex. Fusion of these two cellular plasma membranes is proportional to the observed luciferase activity. Likewise, the effects of scanning mutagenesis of gp41 on entry of the virus into receptor cells were assayed by a luciferase-based assay in which viral entry is proportional to the observed luciferase activity. As shown in Figures 2 and 3 and summarized in Tables 1 and 2, the effects of the mutations range from near complete abolishment to no effect on fusion activity to significantly enhanced activity (HXB2 only). Pictorial representations of the results of both of the functional assays, cell–cell fusion and viral entry, are depicted in Figure 10 to display the position in the helices colored for functional level.

**Mutant Expression, gp160 Proteolytic Processing, and gp120–gp41 Association Effects.** The effects of gp41 mutations on function could be the result of a variety of factors. For example, mutations could have deleterious effects on (a) gp160 expression or the trafficking of the gp160 protein through the endoplasmic reticulum, Golgi apparatus, to the plasma membrane, (b) proteolytic processing of precursor gp160 to the gp41–gp120 complex by furin cleavage, (c) gp41–gp120 association, or (d) a defect in fusogenicity. We tested which of these steps was influenced using Western blot quantification of both the cell lysates and the virus stocks. The results of the Western blot analysis on cell lysates used for cell–cell fusion are summarized in the left halves of Tables 1 and 2. In the right halves of Tables 1 and 2, the results for protein levels on the virus are summarized. The protein levels for the cell lysates for both cell–cell fusion and viral production are shown in Figures 4–7. The expression level of the virus-producing cells could have an effect on resulting protein levels on the virus surface. Finally, quantification of the Western blot analysis for levels of gp120 and gp41 on the virus is shown in Figures 8 and 9.

## DISCUSSION

**Comparison of Cell–Cell Fusion and Viral Entry in HXB2.** Our results reveal several differences between cell–cell fusion and viral entry levels in the case of strain HXB2. In general, viral entry is much less affected by mutation to alanine,

with 21 of the 37 mutation sites reduced to a much greater extent in cell–cell fusion than in viral entry levels (Figure 2). In fact, there are no mutations in HXB2 that exhibit viral entry levels of approximately <50%. Interestingly, many of the substitutions in HXB2 resulted in cell–cell fusion and viral entry levels that are higher than the WT level. Enhanced cell–cell fusion in the case of HXB2 correlated with an increased amount of gp41 as compared to precursor gp160 or the binding partner gp120 in the following instances: N624A, T639A, E648A, Q653A, and E654A. This suggests the intriguing possibility that excess gp41 on the cell surface may facilitate fusion pore formation at the plasma membrane. Of this group of five mutations that are enhanced in cell–cell fusion, four of them are also substantially enhanced with respect to viral entry as well: N624A, T639A, Q653A, and E654A. In the case of viral entry, however, the level of gp41 on the virus is not substantially different from the level of gp120, so it is unlikely that unbound gp41 would be the cause for enhancement of viral entry. One of the mutations with enhanced function, N624A, has a dramatic decrease in the level of expression of gp160. In this case, there is only a slight decrease in the amount of gp41–gp120 complex that the virus incorporates despite the level of gp160 expression being only 45% of the WT level in the producer cell line. The levels of gp120 and gp41 in the producer cell line are much closer to those of the WT (80–100%). Similarly, for mutations W623A, H625A, and T626A, the level of gp160 expression is ~45%; however, the amount of gp120 and gp41 on the virus is 80%, and the function is near WT levels. Viral entry in the cases of T639A and E654A is enhanced, although the gp120 and gp41 levels are the same as that of the WT.

There is an interesting region in HXB2 (S640A through I646A) in which alanine substitutions result in cell–cell fusion levels that are dramatically decreased while the level of viral entry remains near WT levels or is substantially increased. In the case of S640A and L641A, there seems to be a loss of gp120 in both the cells used in the cell–cell fusion assay and the cells used for virus production (Figures 4 and 6). I642A has a clear defect in the proteolytic processing of gp160 to the gp120–gp41 complex in the cells used for cell–cell fusion and virus production. H643A, S644A, L645A, and I646A have partially decreased levels of gp120 and gp41 in both cells producing virus and those used for cell–cell fusion (Figures 4 and 6).

Table 1. HXB2 Envelope Protein Quantification<sup>a</sup>

residue	gp120 expression	gp41 expression	cell–cell fusion (%)	gp120 level	gp41 level	viral entry (%)
W623A	++++	++++	97	++++	+++	90
N624A	++++	++++	136	++++	+++	121
H625A	++++	++++	108	++++	+++	108
T626A	++++	++++	100	++++	++++	90
T627A	+	+	10	+++	+++	49
W628A	+	+	7	++	++	47
M629A	+	+	15	++	++	48
E630A	+	+	15	+++	+++	70
W631A	+	+	5	+	+	68
D632A	+	+	17	+	+	78
R633A	++	++	45	++++	+++	88
E634A	++	++	20	+++	+++	70
I635A	+++	++++	40	++++	+++	95
N636A	++	++	29	+++	+++	72
N637A	++++	++++	108	++++	++++	144
Y638A	++++	++++	113	++++	+++	146
T639A	++++	++++	113	++++	++++	131
S640A	+++	++++	63	++++	++++	122
L641A	+++	++++	62	++++	++++	149
I642A	+	+	13	++++	++++	106
H643A	+++	+++	62	++++	++++	142
S644A	+++	+++	12	++++	++++	118
L645A	+++	+++	18	++++	++++	143
I646A	+++	+++	13	++++	++++	111
E647A	++++	++++	99	++++	++++	144
E648A	++++	++++	122	++++	++++	97
S649A	+++	++++	71	++++	++++	118
Q650A	+++	++++	63	++++	++++	116
N651A	+++	++++	48	++++	++++	108
Q652A	+++	++++	56	++++	++++	120
Q653A	++++	++++	159	++++	++++	116
E654A	++++	++++	177	++++	++++	162
K655A	++++	++++	102	++++	++++	117
N656A	+++	+++	51	++	++	47
E657A	++++	++++	151	++++	++++	141
Q658A	++++	++++	95	++++	++++	110
E659A	++++	++++	119	++++	++++	109

<sup>a</sup>The left-hand side shows protein levels in the cell lysates used for cell–cell fusion. The right-hand side shows protein levels on the virus. Protein levels of expression and incorporation are as follows: +, 0–20% of WT levels; ++, 20–50% of WT levels; +++, 50–80% of WT levels; +++++, >80% of WT levels; and ++++++, >120% of WT levels.

Despite differences in expression levels, the levels of both gp120 and gp41 on the virus are relatively stable, both being >80% in all cases (Figure 8). This dramatic difference between the effects of alanine substitution on viral entry versus cell–cell fusion is most likely due to the propensity for the virus to incorporate the envelope complex with the properly cleaved and associated gp120–gp41 complex. Whereas the cell surface will contain uncleaved gp160, along with any dissociated gp41 that has lost its association with gp120, the population of properly cleaved and associated gp120–gp41 complex is only a small part of the total envelope.

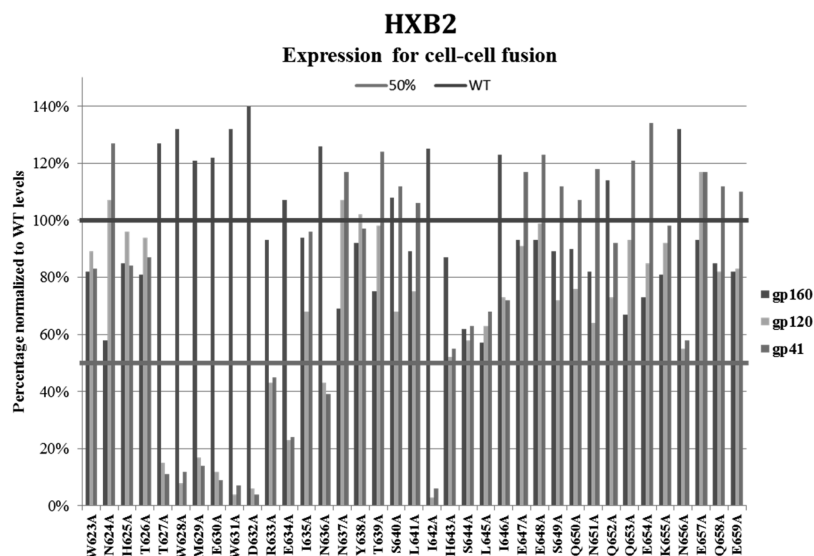
**Mutations in the Hydrophobic Pocket Binding Domain.** HXB2 is generally quite robust to mutation; however, this strain does seem to be particularly vulnerable in the region from T627A to N636A. This region encompasses a

Table 2. JRFL Envelope Protein Quantification<sup>a</sup>

residue	gp120 expression	gp41 expression	cell–cell fusion (%)	gp120 level	gp41 level	viral entry (%)
W623A	+	+	2	+	+	2
N624A	++++	++++	30	++	++	35
N625A	++++	++++	35	++	++	24
M626A	++	++	33	++	++	21
T627A	+	+	9	+	+	8
W628A	+	+	1	+	+	1
M629A	++++	++++	45	++	++	40
E630A	++++	++++	52	++	++	39
W631A	++	++	1	+	++	1
E632A	+	+	60	+	++	31
R633A	+	+	16	+	+	16
E634A	++	+++	69	+	+	58
I635A	++	++	1	+	+	1
D636A	+	++	45	+	+	34
N637A	+++	+++	73	+	+	34
Y638A	++++	++++	40	+	+	47
T639A	+++	+++	68	+	+	47
S640A	+	++	47	+	+	61
E641A	++	++	1	+	+	2
I642A	+++	++++	19	+	+	1
Y643A	+++	++++	12	+	+	38
T644A	++++	++++	73	+	+	11
L645A	+++	++++	5	+	+	6
I646A	++++	++++	29	+	+++	29
E647A	++	++	36	+	+	36
E648A	+	++	26	+	+	30
S649A	+++	+++	33	+	+	33
Q650A	++++	++++	30	+	+	30
N651A	++++	++++	115	++++	++++	90
Q652A	++++	++++	112	++++	++++	102
Q653A	++++	++++	52	+	+	52
E654A	++++	++++	105	+	+	75
K655A	++++	++++	93	+	+	3
N656A	++++	++++	37	+	+	37
E657A	++++	++++	24	++	++	21
Q658A	++	++	0	+	+	9
E659A	+	+	19	+	+	1

<sup>a</sup>The left-hand side shows protein levels in the cell lysates used for cell–cell fusion. The right-hand side shows protein levels on the virus. Protein levels of expression and incorporation are as follows: +, 0–20% of WT levels; ++, 20–50% of WT levels; +++, 50–80% of WT levels; +++++, >80% of WT levels; ++++++, >120% of WT levels.

sequence that is important to the association of the NHR with the CHR in the formation of the core of the 6HB conformation of gp41 that facilitates membrane fusion.<sup>33,34</sup> In the CHR, residues W628, W631, and I635 represent three key hydrophobic residues that bind to an important region in the NHR called the hydrophobic pocket.<sup>35</sup> There is also a critical salt bridge between D632 on the CHR and K574 on the NHR.<sup>36</sup> Mutations in this region substantially decrease the level of cell–cell fusion. The level of viral entry is also decreased, although not as dramatically. This is the only sequence in HXB2 with more than one amino acid in a row that is affected in viral entry. For residues 627–632, it is apparent in the Western blot analysis that the level of gp160 expression is increased over WT levels but that very little cleaved gp120–gp41 complex is apparent (Figure 4). This would suggest that the low level of cell–cell fusion and the decrease in the level of viral entry in



**Figure 4.** Western blot quantification of gp160, gp120, and gp41 levels from HXB2 envelope transfection into 293T cells for cell–cell fusion. The results are presented as a percentage of the WT infrared fluorescence intensity.

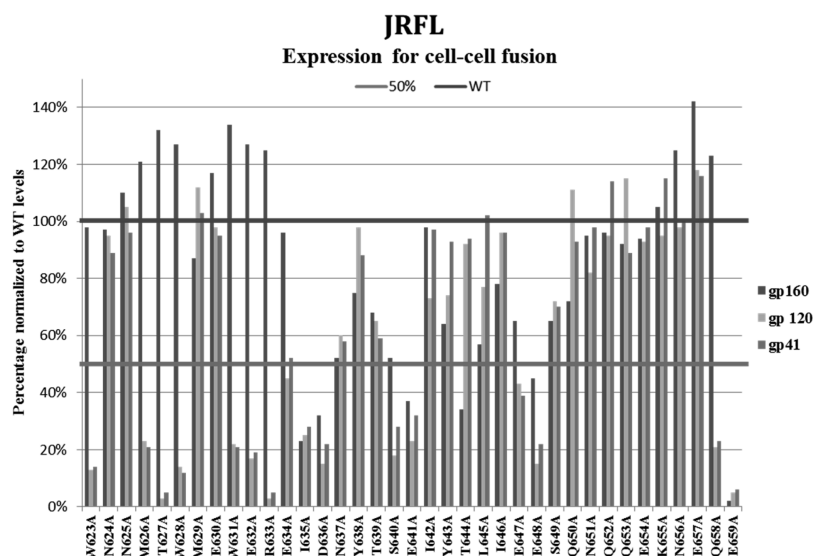


**Figure 5.** Western blot quantification of gp160, gp120, and gp41 levels from JRFL envelope transfection into 293T cells for cell–cell fusion. The results are presented as a percentage of the WT infrared fluorescence intensity.

this region are caused by a defect in the proteolytic processing of precursor gp160 into the noncovalent active gp120–gp41 complex. For residues T627–E630, despite the low level of cleavage, there is approximately 40–50% incorporation of cleaved gp120–gp41 complex incorporated into the virus particle. Interestingly, this would suggest a highly functioning selection process for the cleaved gp120–gp41 complex. In the case of W631A and D632A, there is very little virus incorporation. However, for these two mutations, the viral entry level is relatively high, between 60 and 80%, suggesting that even a small amount of envelope can promote viral entry. It is also interesting to note that in the case of D632, the relatively conservative mutation to alanine decreases the level of viral entry to only 78%, whereas when this residue is switched to the opposite charge, viral entry is abolished.<sup>36</sup> Even mutation to valine, which is more hydrophobic than alanine, causes abrogation of viral entry, whereas alanine does not.<sup>36</sup> In the

case of alanine substitutions between positions 627 and 632, the major defect seems to be in proteolytic cleavage.

**Comparison of Cell–Cell Fusion and Viral Entry in Strain JRFL.** The difference between cell–cell fusion and viral entry was not as dramatic in the case of strain JRFL. Both cell–cell fusion and viral entry were affected to a much greater extent, with the levels of all but 11 sites reduced to <50% in both assays. Only two mutation sites in strain JRFL had WT levels in the cell–cell fusion and viral entry assays, and only four total sites had WT levels in cell–cell fusion. Although with strain JRFL, as opposed to strain HXB2, the difference between cell–cell fusion and viral entry was much less dramatic, the level of cell–cell fusion was more often higher than the level of viral entry compared to the WT levels in each case. In contrast, the level of cell–cell fusion was lower than the level of viral entry in only two cases (S640A and Y643A). In fact, the level of cell–cell fusion was much greater in four cases: E632A, N637A, T644A, and K655A. In comparison to this effect seen with

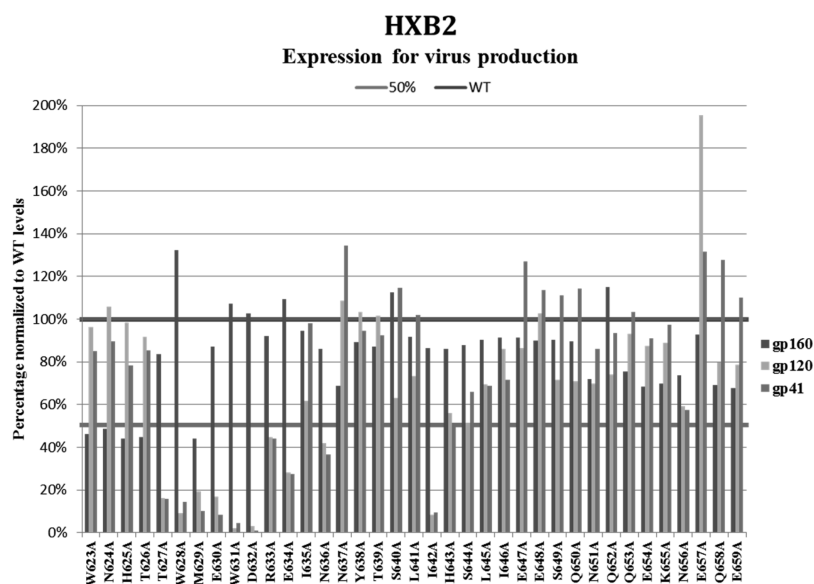


**Figure 6.** Western blot quantification of gp160, gp120, and gp41 levels from HXB2 envelope transfection into 293T cells for virus production. The results are presented as a percentage of the WT infrared fluorescence intensity.

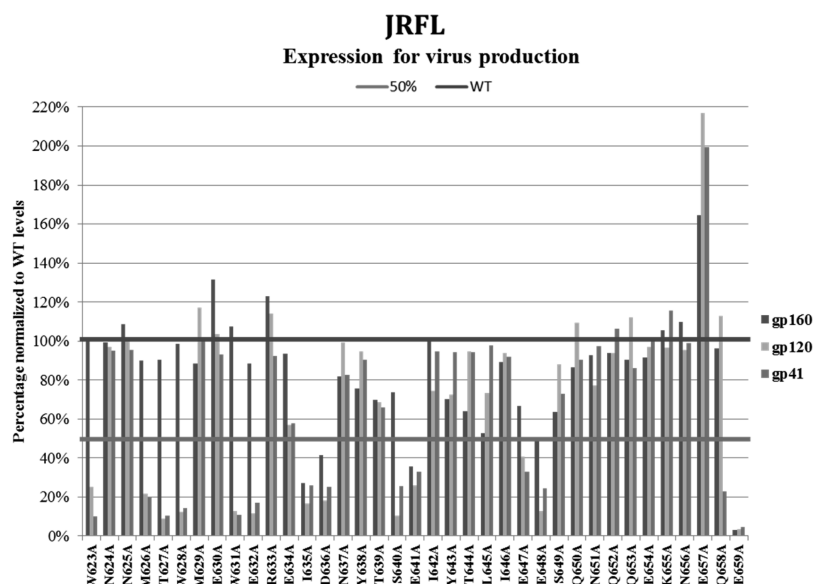


**Figure 7.** Western blot quantification of gp160, gp120, and gp41 levels from JRFL envelope transfection into 293T cells for virus production. The results are presented as a percentage of the WT infrared fluorescence intensity.

strain JRFL, there is no case in which the level of cell–cell fusion is dramatically higher than the level of viral entry for strain HXB2. This suggests that strain HXB2 is markedly robust at assembly and produces functional virus despite defects in expression and/or proteolytic processing of gp160 to the gp120–gp41 complex. This observation is consistent with the fact that strain HXB2 is a highly lab-adapted strain.<sup>37,38</sup>

Another interesting issue with strain JRFL is that several mutational sites have a functional defect in cell–cell fusion, whereas the upstream events, including expression, proteolytic cleavage, and gp120–gp41 association, do not appear to be affected. These residues are N624A, N625A, M629A, E630A, Y638A, T644A, I646A, Q653A, N656A, and E657A. The level of incorporation into the virus is relatively low for all of these sites, and therefore, the defect in viral entry is likely due to a

combination of effects on incorporation as well as six-helix bundle formation.

**Comparison between Strains HXB2 and JRFL.** Our mutagenesis study is the first conducted using side-by-side scanning of two different viral isolates each with different coreceptor usage: HXB2 is CXCR4-utilizing, and JRFL is CCR5-utilizing. Our results show a distinct difference between the two strains. JRFL is much more vulnerable both in cell–cell fusion and in viral entry studies to single-amino acid substitution with alanine than is HXB2.

Most mutagenesis studies to date have focused on strain HXB2. In the case of strain HXB2, it is most common to see a defect in incorporation that coincides with a cleavage defect (T627A, W628A, M629A, E630A, W631A, E632A, R633A, E634A, I635A, N636A, N637A, Y638A, T639A, and L641A).

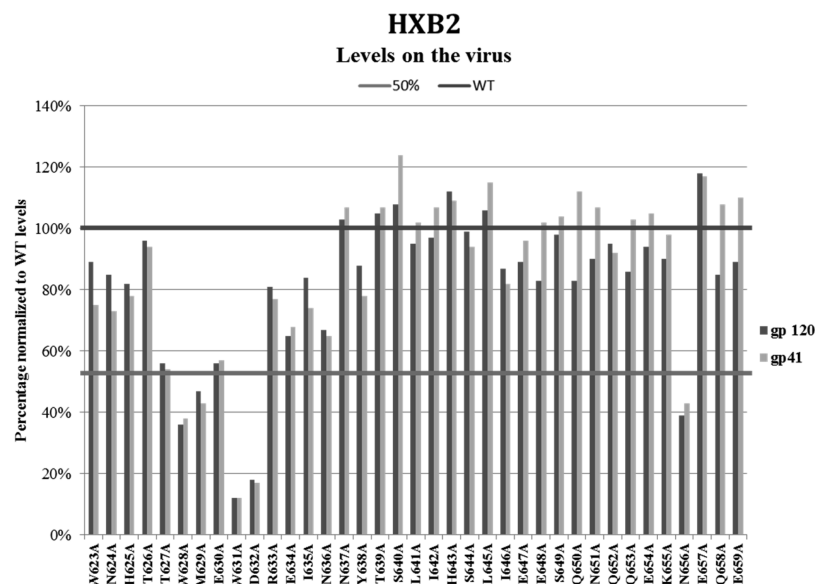


**Figure 8.** Western blot quantification of gp120 and gp41 levels on the HXB2 virus. The results are presented as a percentage of the WT infrared fluorescence intensity.

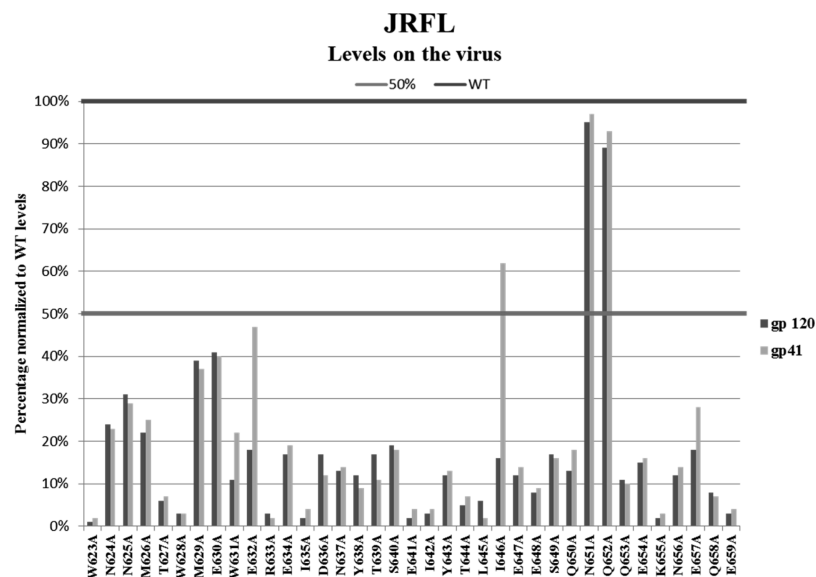


**Figure 9.** Western blot quantification of gp120 and gp41 levels on JRFL virus. The results are presented as a percentage of the WT infrared fluorescence intensity.

One of the most surprising results of our study, however, was that many of the alanine substitutions in strain JRFL resulted in a cleavage defect that was nonetheless incorporated into the virus as full-length gp160. This is true despite the fact that the region that we are scanning, namely the CHR, is at the opposite end of the ectodomain from the cleavage site, which is located at the extreme N-terminus of gp41. Long-range effects on function can occur when a mutation in one region affects the local secondary structure. This in turn affects the region's ability to associate with other regions to form the tertiary or quaternary structure necessary for proper function. This type of long-range effect has been observed previously for single-amino acid substitutions.<sup>29,39</sup> However, it has not been commonly observed for the virus to incorporate uncleaved gp160, which is indeed what we see in strain JRFL for multiple residues (W623A, N624A, N625A, M626A, T627A, W628A,

M629A, E630A, W631A, E632A, R633A, E634A, I635A, E641A, I642A, T644A, L645A, I646A, E647A, E648A, S649A, Q650A, N651A, Q652A, Q653A, E654A, K655A, N656A, E657A, Q658A, and E659A). This suggests that the viral process of selecting for the functional cleaved envelope trimer is not as robust in strain JRFL as in lab-adapted strain HXB2 for which we see robust levels of the gp120–gp41 complex on the virus despite dramatic defects in expression and/or cleavage of gp160.

There could be many factors underlying the potential for differences between strains HXB2 and JRFL. Miyauchi et al. in visualizing retrovirus uptake found that strain JRFL has a much higher propensity to dissociate from cells and hence is less efficient at entering cells than is strain HXB2.<sup>16</sup> It is possible that this lowered efficiency contributes to the sensitivity of JRFL to alanine substitution. Strain JRFL has also been found



**Table 3. Published Results for Alanine Substitutions Performed in the CHR Region of gp41**

residue	isolate	published results
W628	HXB2	impaired precursor cleavage, abrogated viral entry level compared to that of the WT <sup>12</sup>
W628	HXB2	expression similar to that of the WT, with a lowered level of cell surface gp120 and a lowered level of syncytium formation compared to those of the WT <sup>11,a</sup>
W631	HXB2	expression similar to that of the WT, with a lowered level of cell surface gp120 and lowered level of syncytium formation compared to those of the WT <sup>11,a</sup>
I635	HXB2	expression similar to that of the WT, with a lowered level of cell surface gp120 and a lowered level of syncytium compared to those of the WT <sup>11,a</sup>
Y638	HXB2	levels of expression on the cell surface, proteolytic processing, gp120 association, and syncytium formation similar to those of the WT despite the level of gp120 shedding being elevated <sup>11,a</sup>
T639	HXB2	no expression, no syncytium formation <sup>41</sup>
I642	HXB2	expression similar to that of the WT, with a lowered level of cell surface gp120 and a lowered level of syncytium formation compared to those of the WT <sup>11,a</sup>
L645	H64333	levels of expression, surface gp120, and syncytium formation similar to those of the WT <sup>11,a</sup>
S649	HXB2	levels of expression, surface gp120, and syncytium formation similar to those of the WT <sup>11,a</sup>
Q652	HXB2	levels of expression, surface gp120, and syncytium formation similar to those of the WT <sup>11,a</sup>

<sup>a</sup>Note that in this study WT levels of syncytium formation were designated to be those between 50 and 120% of that of the wild type.

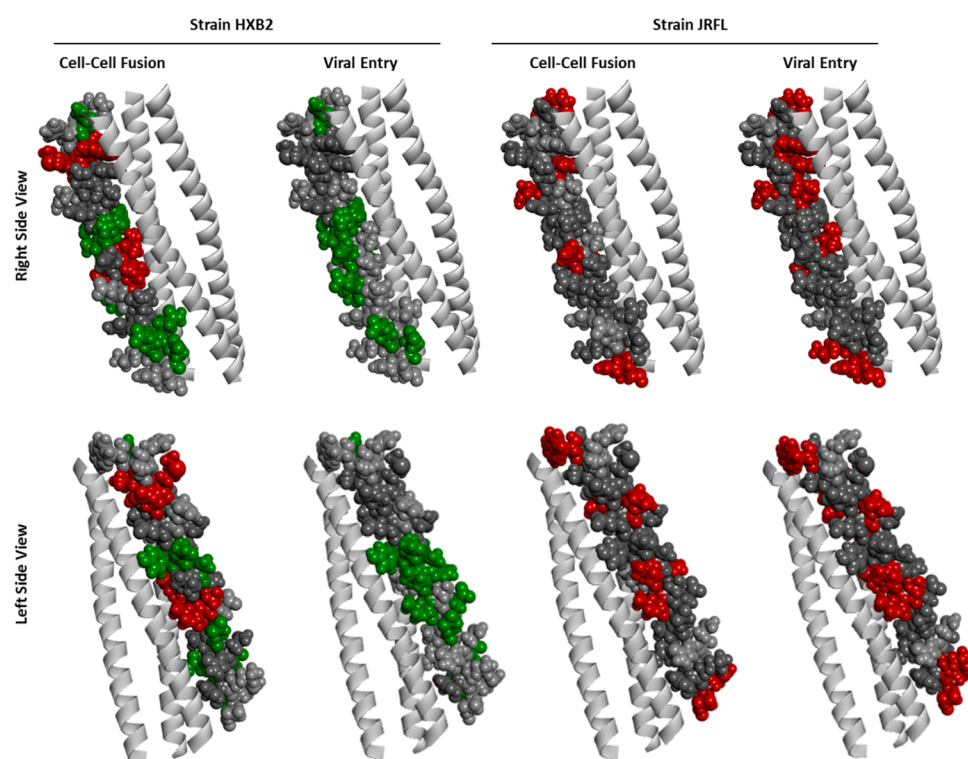


**Figure 10.** Molecular models highlighting the functionality of mutations in the HIV gp41 CHR. The inner NHR helical bundle is shown as a gray ribbon diagram. The top of the structure is that which is oriented toward the loop region. The top panel of models is a view of the right side of the CHR helix. The bottom panel is a view that is flipped about the vertical access to display the left side of the CHR helix. Only one of the CHR peptides is shown for the sake of simplicity. Amino acid residues without highlighting (light gray) have levels of 80–120% of either cell–cell fusion or viral entry as indicated. Those colored green have levels increased above 120% of the WT level. Those colored dark gray have levels diminished to 20–50% of the WT level, and those colored red have levels diminished to <20% of the WT level. The structure was rendered with Discovery Studios Visualizer based upon coordinates from the theoretical model of Protein Data Bank entry 1IF3 with HIV HXB2 as the sequence.<sup>4</sup>

to have unusually efficient gp160 proteolytic processing.<sup>40</sup> However, in our studies, both strains have a similar number of alanine substitution mutations with clear cleavage defects (7 in JRFL and 10 in HXB2). Therefore, efficient proteolytic processing of gp160 to the gp120–gp41 complex in strain JRFL does not seem to make up for defects seen with these mutations.

**Comparison with Previously Published Alanine Substitutions in the CHR.** A summary of previously published results for mutagenesis to alanine in this region is shown in Table 3. To the best of our knowledge, mutations to

date have been studied only in strain HXB2. The W628A mutation showed impaired precursor cleavage in agreement with our results;<sup>12</sup> however, viral entry was completely abrogated, whereas in our case, the level of viral entry was reduced to ~50%. W628A was also studied by another group but only in the formation of syncytia.<sup>11</sup> In this case, cell–cell fusion was abrogated, which is in agreement with our results (<10%). This study found a high level of gp120 shedding, whereas the largest defect of this mutation from our Western blot analysis would seem to be a defect in precursor cleavage. Surprisingly, despite the cleavage defect, the virus is able to

incorporate almost 40% of the WT level of gp41, which seems to be in a 1:1 stoichiometry with gp120 on the virus surface. W631A exhibited the same results in the syncytium formation assay with abrogated cell–cell fusion and gp120 shedding. Again, our results suggest that there is a defect in furin cleavage. In this case, however, the virus has levels of gp41 and gp120 of <20%. The viral entry level, however, is higher (68%). I635A exhibited a decreased level of syncytium formation, in agreement with our results. Indeed, we also see a decrease in the amount of gp120 as compared to the amount of gp41. On the virus, however, this effect is diminished, suggesting that the virus preferentially incorporates the associated gp41–gp120 complex as opposed to unbound gp41. Hence, viral entry levels are near WT levels. With Y638A, researchers found a lowered level of gp120; however, the level of syncytium formation was near the WT level.<sup>11</sup> In comparison, our results for both cell–cell fusion and viral entry were at or above WT levels. With this mutation, we found levels of both gp41 and gp120 near WT levels in all Western blot analyses. In the case of the T639A mutation, previous research revealed no expression on the cell surface and a lowered level of syncytium formation.<sup>41</sup> We saw a partially lowered level of gp160 expression; however, the virus had WT levels of both proteins. Levels of both cell–cell fusion as measured by the luciferase assay and viral entry were near WT levels. I642A similarly showed a decreased level of syncytium formation with gp120 shedding.<sup>11</sup> With this mutation, we found a very dramatic cleavage defect with gp41 and gp120 levels at <10%. Again strikingly, the virus had WT levels of both proteins, and the level of viral entry was near that of the WT. The level of cell–cell fusion, however, was drastically reduced with the envelope protein on cells being made up overwhelmingly of uncleaved gp160. It is likely that this overwhelming concentration of uncleaved gp160 interferes with the fusion capacity of the very small amount of cleaved protein on the cell surface. For mutations L645A, S649A, and Q652A, the results are similar between our study and previous results.<sup>11</sup> However, we see a diminution in the level of cell–cell fusion with L645A at 20% and Q652 at 55%. Otherwise, these mutations exhibit protein levels that are near the WT level and viral entry levels greater than the WT level.

**Structural Implications.** Molecular models of the CHR domains in the presence of the N-helical inner bundle of the 6HB structure of gp41 are shown in Figure 10. Most surprisingly, mutations that abrogate fusion and/or entry are not isolated to the hydrophobic pocket region, nor are the deleterious mutations isolated to one face of the helix as might be expected because of interference with CHR–NHR association. This could simply suggest the vulnerability of HIV gp41 to long-range effects of manipulation. However, it also suggests that there are other structural conformations upstream of the postfusion structure that have different interactions and potentially also secondary structure and cannot be depicted by models of the 6HB of gp41. Another observation is that mutations that enhance infectivity in strain HXB2 are generally not located at the ends of the CHR. In the case of strain JRFL, it is readily apparent in this depiction how vulnerable this strain is to mutation. Also, both of the CHR termini are diminished, and the results for cell–cell fusion in comparison to viral entry are much more similar than those in strain HXB2. Finally, the amino acid positions that are unchanged (light gray) can be considered as reasonable candidates for manipulation to facilitate labeling for structural studies.

The alanine scanning mutagenesis reported herein reveals new insights into the individual contributions of the amino acids of the CHR of gp41 and intriguing differences between strains and between the phenomena of cell–cell fusion and viral entry. Most importantly, these data give us a starting point for the development of tools to better characterize the different conformations of gp41 by a combination of mutagenesis, biochemistry, and structural biology techniques.

These studies suggest that the HIV envelope is sensitive to mutation in a strain-dependent manner. Some strains are dramatically more sensitive than others, which is proven by the differences in sensitivity to mutation between strains HXB2 and JRFL. The dramatic differences between cell–cell fusion and viral entry also lend support to the possibility that there are mechanistic differences between these two phenomena. These data also confirm evidence of the importance of the gp41 CHR regions to envelope function and provide insight into areas within the protein sequence that potentially can be manipulated for labeling purposes while retaining function.

## AUTHOR INFORMATION

### Corresponding Author

\*Address: 109 BRB, 3435 Main St., Buffalo, NY 14214. E-mail: ajacobs2@buffalo.edu. Telephone: (716) 829-2087. Fax: (716) 829-2111.

### Funding

This work was supported by startup funds from the University at Buffalo School of Medicine and Biomedical Sciences. This work was supported in part by the University of Rochester Developmental Center for AIDS Research (National Institutes of Health Grant P30AI078498).

### Notes

The authors declare no competing financial interest.

## ACKNOWLEDGMENTS

The following reagents were obtained through the NIH AIDS Research and Reference Reagent Program, Division of AIDS, National Institute of Allergy and Infectious Diseases, NIH: TZM-bl from Dr. John C. Kappes, Dr. Xiaoyun Wu, and Tranzyme Inc.,<sup>42</sup> U87.CD4.CXCR4 from Dr. HongKui Deng and Dr. Dan R. Littman,<sup>43</sup> pNL4-3.HSA.R-E- and pNL4-3.Luc.R-E- from Dr. Nathaniel Landau,<sup>30</sup> pHXB2-env from Dr. Kathleen Page and Dr. Dan Littman,<sup>44</sup> HIV-1 gp41 Hybridoma (Chessie 8) from Dr. George K. Lewis, the HIV-1 p24 hybridoma (183-H12-5C) from Dr. Bruce Chesebro and Dr. Hardy Chen,<sup>45</sup> pCMV-rev from Dr. Marie-Louise Hammarström and Dr. David Rekosh,<sup>27</sup> and pCEP4-Tat from Dr. Lung-Ji Chang.<sup>28</sup> pCAGGS JRFL gp160 WT was a gift from Dr. James Binley.

## REFERENCES

- (1) Jacobs, A., Simon, C., and Caffrey, M. (2006) Thermostability of the HIV gp41 wild-type and loop mutations. *Protein Pept. Lett.* 13, 477–480.
- (2) Melikyan, G. B., Markosyan, R. M., Hemmati, H., Delmedico, M. K., Lambert, D. M., and Cohen, F. S. (2000) Evidence that the transition of HIV-1 gp41 into a six-helix bundle, not the bundle configuration, induces membrane fusion. *J. Cell Biol.* 151, 413–423.
- (3) Jiang, S., Lin, K., Strick, N., and Neurath, A. R. (1993) Inhibition of HIV-1 infection by a fusion domain binding peptide from the HIV-1 envelope glycoprotein GP41. *Biochem. Biophys. Res. Commun.* 195, 533–538.

- (4) Mkrtchyan, S. R., Markosyan, R. M., Eadon, M. T., Moore, J. P., Melikyan, G. B., and Cohen, F. S. (2005) Ternary complex formation of human immunodeficiency virus type 1 Env, CD4, and chemokine receptor captured as an intermediate of membrane fusion. *J. Virol.* 79, 11161–11169.
- (5) Wild, C., Oas, T., McDaniel, C., Bolognesi, D., and Matthews, T. (1992) A synthetic peptide inhibitor of human immunodeficiency virus replication: Correlation between solution structure and viral inhibition. *Proc. Natl. Acad. Sci. U.S.A.* 89, 10537–10541.
- (6) Matthews, T., Salgo, M., Greenberg, M., Chung, J., DeMasi, R., and Bolognesi, D. (2004) Enfuvirtide: The first therapy to inhibit the entry of HIV-1 into host CD4 lymphocytes. *Nat. Rev. Drug Discovery* 3, 215–225.
- (7) Wild, C., Greenwell, T., Shugars, D., Rimsky-Clarke, L., and Matthews, T. (1995) The inhibitory activity of an HIV type 1 peptide correlates with its ability to interact with a leucine zipper structure. *AIDS Res. Hum. Retroviruses* 11, 323–325.
- (8) Chan, D. C., Fass, D., Berger, J. M., and Kim, P. S. (1997) Core structure of gp41 from the HIV envelope glycoprotein. *Cell* 89, 263–273.
- (9) Tan, K., Liu, J., Wang, J., Shen, S., and Lu, M. (1997) Atomic structure of a thermostable subdomain of HIV-1 gp41. *Proc. Natl. Acad. Sci. U.S.A.* 94, 12303–12308.
- (10) Weissenhorn, W., Dessen, A., Harrison, S. C., Skehel, J. J., and Wiley, D. C. (1997) Atomic structure of the ectodomain from HIV-1 gp41. *Nature* 387, 426–430.
- (11) Wang, S., York, J., Shu, W., Stoller, M. O., Nunberg, J. H., and Lu, M. (2002) Interhelical Interactions in the gp41 Core: Implications for Activation of HIV-1 Membrane Fusion. *Biochemistry* 41, 7283–7292.
- (12) Weng, Y., Yang, Z., and Weiss, C. D. (2000) Structure-Function Studies of the Self-Assembly Domain of the Human Immunodeficiency Virus Type 1 Transmembrane Protein gp41. *J. Virol.* 74, 5368–5372.
- (13) Caffrey, M., Cai, M., Kaufman, J., Stahl, S. J., Wingfield, P. T., Covell, D. G., Gronenborn, A. M., and Clore, G. M. (1998) Three-dimensional solution structure of the 44 kDa ectodomain of SIV gp41. *EMBO J.* 17, 4572–4584.
- (14) Caffrey, M. (2001) Model for the structure of the HIV gp41 ectodomain: Insight into the intermolecular interactions of the gp41 loop. *Biochim. Biophys. Acta* 1536, 116–122.
- (15) Neurath, A. R., Strick, N., and Jiang, S. (1992) Synthetic peptides and anti-peptide antibodies as probes to study interdomain interactions involved in virus assembly: The envelope of the human immunodeficiency virus (HIV-1). *Virology* 188, 1–13.
- (16) Miyauchi, K., Marin, M., and Melikyan, G. B. (2010) Visualization of retrovirus uptake and delivery into acidic endosomes. *Biochem. J.* 434, 559–569.
- (17) Page, K. A., Landau, N. R., and Littman, D. R. (1990) Construction and use of a human immunodeficiency virus vector for analysis of virus infectivity. *J. Virol.* 64, 5270–5276.
- (18) Krell, T., Greco, F., Engel, O., Dubayle, J., Kennel, A., Charlotiaux, B., Brasseur, R., Chevalier, M., Sodoyer, R., and El Habib, R. (2004) HIV-1 gp41 and gp160 are hyperthermostable proteins in a mesophilic environment. Characterization of gp41 mutants. *Eur. J. Biochem.* 271, 1566–1579.
- (19) Jiang, S., Lin, K., Strick, N., and Neurath, A. R. (1993) HIV-1 inhibition by a peptide. *Nature* 365, 113.
- (20) Lu, M., Blacklow, S. C., and Kim, P. S. (1995) A trimeric structural domain of the HIV-1 transmembrane glycoprotein. *Nat. Struct. Biol.* 2, 1075–1082.
- (21) Buzon, V., Natrajan, G., Schibli, D., Campelo, F., Kozlov, M. M., and Weissenhorn, W. (2010) Crystal structure of HIV-1 gp41 including both fusion peptide and membrane proximal external regions. *PLoS Pathog.* 6, e1000880.
- (22) Miyauchi, K., Kim, Y., Latinovic, O., Morozov, V., and Melikyan, G. B. (2009) HIV enters cells via endocytosis and dynamin-dependent fusion with endosomes. *Cell* 137, 433–444.
- (23) Konopka, K., Pretzer, E., Celada, F., and Duzgunes, N. (1995) A monoclonal antibody to the gp120-CD4 complex has differential effect on HIV-induced syncytium formation and viral infectivity. *J. Gen. Virol.* 76 (Part 3), 669–679.
- (24) Yee, M., Konopka, K., Balzarini, J., and Duzgunes, N. (2011) Inhibition of HIV-1 Env-Mediated Cell-Cell Fusion by Lectins, Peptide T-20, and Neutralizing Antibodies. *Open Virol. J.* 5, 44–51.
- (25) Platt, E. J., Wehrly, K., Kuhmann, S. E., Chesebro, B., and Kabat, D. (1998) Effects of CCR5 and CD4 cell surface concentrations on infections by macrophagetropic isolates of human immunodeficiency virus type 1. *J. Virol.* 72, 2855–2864.
- (26) Schulke, N., Vesanen, M. S., Sanders, R. W., Zhu, P., Lu, M., Anselma, D. J., Villa, A. R., Parren, P. W., Binley, J. M., Roux, K. H., Maddon, P. J., Moore, J. P., and Olson, W. C. (2002) Oligomeric and conformational properties of a proteolytically mature, disulfide-stabilized human immunodeficiency virus type 1 gp140 envelope glycoprotein. *J. Virol.* 76, 7760–7776.
- (27) Lewis, N., Williams, J., Rekosh, D., and Hammarskjöld, M. L. (1990) Identification of a cis-acting element in human immunodeficiency virus type 2 (HIV-2) that is responsive to the HIV-1 rev and human T-cell leukemia virus types I and II rex proteins. *J. Virol.* 64, 1690–1697.
- (28) Chang, L. J., Ullrich, V., Iwakuma, T., Cui, Y., and Zucali, J. (1999) Efficacy and safety analyses of a recombinant human immunodeficiency virus type 1 derived vector system. *Gene Ther.* 6, 715–728.
- (29) Sen, J., Jacobs, A., and Caffrey, M. (2008) Role of the HIV gp120 conserved domain 5 in processing and viral entry. *Biochemistry* 47, 7788–7795.
- (30) He, J., Choe, S., Walker, R., Di Marzio, P., Morgan, D., and Landau, N. (1995) Human immunodeficiency virus type 1 viral protein R (Vpr) arrests cells in the G2 phase of the cell cycle by inhibiting p34cdc2 activity. *J. Virol.* 69, 6705–6711.
- (31) Yi, H. A., Diaz-Aguilar, B., Bridon, D., Quraishi, O., and Jacobs, A. (2011) Permanent Inhibition of Viral Entry by Covalent Entrapment of HIV gp41 on the Virus Surface. *Biochemistry* 50, 6966–6972.
- (32) Abacioglu, Y. H., Fouts, T. R., Laman, J. D., Claassen, E., Pincus, S. H., Moore, J. P., Roby, C. A., Kamin-Lewis, R., and Lewis, G. K. (1994) Epitope mapping and topology of baculovirus-expressed HIV-1 gp160 determined with a panel of murine monoclonal antibodies. *AIDS Res. Hum. Retroviruses* 10, 371–381.
- (33) Wang, H., Qi, Z., Guo, A., Mao, Q., Lu, H., An, X., Xia, C., Li, X., Debnath, A. K., Wu, S., Liu, S., and Jiang, S. (2009) ADS-J1 inhibits human immunodeficiency virus type 1 entry by interacting with the gp41 pocket region and blocking fusion-active gp41 core formation. *Antimicrob. Agents Chemother.* 53, 4987–4998.
- (34) Yu, X., Lu, L., Cai, L., Tong, P., Tan, S., Zou, P., Meng, F., Chen, Y. H., and Jiang, S. (2012) Mutations of Gln64 in the HIV-1 gp41 N-terminal heptad repeat render viruses resistant to peptide HIV fusion inhibitors targeting the gp41 pocket. *J. Virol.* 86, 589–593.
- (35) Chan, D. C., Chutkowski, C. T., and Kim, P. S. (1998) Evidence that a prominent cavity in the coiled coil of HIV type 1 gp41 is an attractive drug target. *Proc. Natl. Acad. Sci. U.S.A.* 95, 15613–15617.
- (36) He, Y., Liu, S., Li, J., Lu, H., Qi, Z., Liu, Z., Debnath, A. K., and Jiang, S. (2008) Conserved salt bridge between the N- and C-terminal heptad repeat regions of the human immunodeficiency virus type 1 gp41 core structure is critical for virus entry and inhibition. *J. Virol.* 82, 11129–11139.
- (37) Daar, E. S., Li, X. L., Moudgil, T., and Ho, D. D. (1990) High concentrations of recombinant soluble CD4 are required to neutralize primary human immunodeficiency virus type 1 isolates. *Proc. Natl. Acad. Sci. U.S.A.* 87, 6574–6578.
- (38) McKeating, J. A., Bennett, J., Zolla-Pazner, S., Schutten, M., Ashelford, S., Brown, A. L., and Balfe, P. (1993) Resistance of a human serum-selected human immunodeficiency virus type 1 escape mutant to neutralization by CD4 binding site monoclonal antibodies is conferred by a single amino acid change in gp120. *J. Virol.* 67, 5216–5225.

- (39) Sen, J., Yan, T., Wang, J., Rong, L., Tao, L., and Caffrey, M. (2010) Alanine scanning mutagenesis of HIV-1 gp41 heptad repeat 1: Insight into the gp120-gp41 interaction. *Biochemistry* 49, 5057–5065.
- (40) Crooks, E. T., Tong, T., Osawa, K., and Binley, J. M. (2011) Enzyme digests eliminate nonfunctional Env from HIV-1 particle surfaces, leaving native Env trimers intact and viral infectivity unaffected. *J. Virol.* 85, 5825–5839.
- (41) Cao, J., Bergeron, L., Helseth, E., Thali, M., Repke, H., and Sodroski, J. (1993) Effects of amino acid changes in the extracellular domain of the human immunodeficiency virus type 1 gp41 envelope glycoprotein. *J. Virol.* 67, 2747–2755.
- (42) Platt, E. J., Wehrly, K., Kuhmann, S. E., Chesebro, B., and Kabat, D. (1998) Effects of CCR5 and CD4 Cell Surface Concentrations on Infections by Macrophage-tropic Isolates of Human Immunodeficiency Virus Type 1. *J. Virol.* 72, 2855–2864.
- (43) Bjorndal, A., Deng, H., Jansson, M., Fiore, J., Colognesi, C., Karlsson, A., Albert, J., Scarlatti, G., Littman, D., and Fenyo, E. (1997) Coreceptor usage of primary human immunodeficiency virus type 1 isolates varies according to biological phenotype. *J. Virol.* 71, 7478–7487.
- (44) Page, K. A., Landau, N. R., and Littman, D. R. (1990) Construction and use of a human immunodeficiency virus vector for analysis of virus infectivity. *J. Virol.* 64, 5270–5276.
- (45) Chesebro, B., Wehrly, K., Nishio, J., and Perryman, S. (1992) Macrophage-tropic human immunodeficiency virus isolates from different patients exhibit unusual V3 envelope sequence homogeneity in comparison with T-cell-tropic isolates: Definition of critical amino acids involved in cell tropism. *J. Virol.* 66, 6547–6554.